Strong and broadband terahertz absorber using SiO_2-based metamaterial structure*

Mo Man-Man(莫漫漫)[a], Wen Qi-Ye(文岐业)[a]†, Chen Zhi(陈 智)[b], Yang Qing-Hui(杨青慧)[a], Qiu Dong-Hong(邱东鸿)[a], Li Sheng(李 胜)[a], Jing Yu-Lan(荆玉兰)[a], and Zhang Huai-Wu(张怀武)[a]

[a] *State Key Laboratory of Electronic Films and Integrated Devices, University of Electronic Science and Technology of China, Chengdu* 610054, *China*

[b] *National Key Laboratory of Science and Technology of Communication. University of Electronic Science and Technology of China, Chengdu* 610054, *China*

(Received 8 August 2013; revised manuscript received 23 August 2013; published online 10 February 2014)

We design and experimentally demonstrate a broadband metamaterial absorber in the terahertz (THz) band based on a periodic array of aluminum (Al) squares with two different sizes. A thin silicon dioxide (SiO_2) film rather than a conventional polyimide (PI) layer is used as a dielectric spacer to separate Al squares from the platinum (Pt) ground plane in our design, which significantly improves the design precision and the feasibility of the device fabrication. The combination of different sizes of Al squares gives rise to an absorption bandwidth of over 210 GHz with an absorption of over 90%. Our results also show that our device is almost polarization-insensitive. It works very well for all azimuthal angles with an absorption of beyond 80%.

Keywords: terahertz, metamaterials, absorption, broadband

PACS: 78.20.Ci, 77.22.Ch, 78.47.–p **DOI:** 10.1088/1674-1056/23/4/047803

1. Introduction

Recently, metamaterial (MM) absorbers in microwave and terahertz (THz) bands have attracted much attention due to the advantages such as high absorption, ultrathin thickness, frequency selectivity, and design flexibility.[1–6] Theoretically, a unity absorptivity can be achieved in such an MM absorber device with a thickness of typically $\lambda/20$ (λ is the working wavelength), which is especially important in the THz band since such a strong and ultrathin absorbing material is difficult to find in nature. Since the first demonstration of an MM absorber at microwave frequency by Landy *et al.*,[5] great efforts have been made to develop THz MM absorbers and to improve the angular and polarization performance.[4,6–11] However, most of the above mentioned absorbers run in a relatively narrow band, which limits the applications, such as in stealth technology or energy harvesting. Broadband THz MM absorbers are highly required.

In our group, we previously proposed a dual-band terahertz absorber which exhibits two strong narrow-band absorptions.[12] Then, it was followed by quite a few studies to develop dual-band or multi-band THz MM absorbers.[13–16] These efforts pave the way to a broadband THz absorber since the absorption band can be expanded by merging several closely positioned resonant peaks in the absorption spectrum. Based on this concept, broadband absorption of the THz MM absorber was numerically investigated and demonstrated experimentally.[17–23] The first experimental realization of a broadband resonant THz MM absorber was conducted by Grant *et al.*[23] by stacking metal–insulator layers with differing structural dimensions. However, the fabrication of such a broadband absorber is very complicated. Another THz absorber with an absorption bandwidth of 100 GHz was experimentally realized by Huang *et al.*,[24] which is somewhat polarization-sensitive and the maximum absorption is only 80%.[24] For both experimental studies, polyimide (PI) layers were used as the separation layers. The PI layer is fabricated by a spin-coating method by multiple steps, thus the thickness uniformity is hard to precisely control. Furthermore, the refractive index of the PI is sensitive to the fabrication process, which inevitably induces a discrepancy between the simulation and measurement results.[23]

In this paper, we experimentally demonstrate a THz broadband absorber using an SiO_2 dielectric spacer. SiO_2 has excellent thermal, mechanical, and dielectric properties.[25] Based on an SiO_2 layer, a narrow-band THz absorber has been previously studied.[26] But an SiO_2 based broadband THz absorber has never been reported. As to the broadband MM absorber derived from combining multiple absorption peaks, the thickness of the dielectric layer is essentially important for the bandwidth. As is well known, the fabrication of SiO_2 films is a typical semiconductor fabrication process. The film thick-

*Project supported by the National Natural Science Foundation of China (Grant No. 61131005), the Key Project of the Chinese Ministry of Education (Grant No. 313013), the New Century Excellent Talent Foundation, China (Grant No. NCET-11-0068), the Sichuan Youth Science and Technology Foundation, China (Grant No. 2011JQ0001), the Specialized Research Fund for the Doctoral Program of Higher Education, China (Grant No. 20110185130002), and the THz Science and Technology Foundation from the China Academy of Engineering Physics, China (Grant No. CAEPTHZ201207).

†Corresponding author. E-mail: qywen@uestc.edu.cn; qywen@163.com

© 2014 Chinese Physical Society and IOP Publishing Ltd

ness can be precisely controlled and the large-area uniformity can also be achieved. All these features make SiO_2 very suitable for a broadband THz MM absorber. In the present work, a thin SiO_2 film rather than a conventional PI layer is used as a dielectric spacer to separate Al squares from a platinum (Pt) ground plan. By incorporating two kinds of Al squares with different sizes into an array, an absorption bandwidth over 210 GHz with an absorption magnitude of 90% is obtained near 2.5 THz. The absorption is only slightly sensitive to the polarization of the THz wave and works very well for a wide azimuthal angle. The experimental results are very consistent with the simulation results, indicating that the adoption of the SiO_2 dielectric layer significantly improves the design precision and the feasibility of the device fabrication.

2. Design and simulation

The MM absorber is a three-layer device with the structure as depicted in Fig. 1. A Pt ground layer is separated from the top Al squares by an SiO_2 spacer. Specially, a structural unit of the absorber is composed of two mixed-size squares as schematically illustrated in Fig. 1(c). The refractive index of SiO_2 is $2.0+0.025i$ at THz frequencies.[27,28] The conductivity values of Al and Pt are 1×10^7 S/m and 9.43×10^6 S/m, respectively. The periodic boundary conditions are set to be along the x- and y-axis directions as indicated in Fig. 1(a). A plane wave is vertically incident on the front face of the structure, and as an excitation source, the electric field is polarized in the direction parallel to the x-axis direction.[15,17,21,29–31] Utilizing the computer simulation technology (CST) microwave studio, the structure of the broadband absorber is optimized by simulating radiation at normal incidence and the obtained size parameters are listed in the captions of Figs. 1(b) and 1(c).

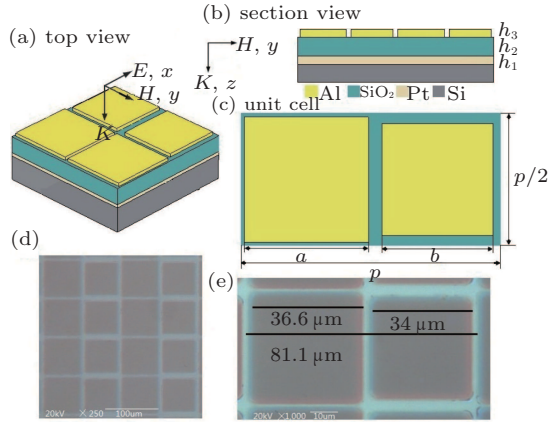


Fig. 1. (color online) Schematic diagram of the broadband THz metamaterial absorber. (a) The top view and (b) the section view of a portion of the designed absorber with $h_1 = 100$ nm, $h_2 = 2$ μm, $h_3 = 100$ nm. (c) A simulated unit cell of the mixed-size square resonator with $a = 36.9$ μm, $b = 34.2$ μm, $p = 80$ μm. (d) Micrograph of a portion of the fabricated absorber. (e) A cell structure of the fabricated absorber with $a = 36.6$ μm, $b = 34$ μm, and $p = 81.1$ μm.

In order to clarify how different narrow-band absorbers are combined to form a broadband absorber, the absorption spectra of three differently configured absorbers, which are shown in the insets of Fig. 2, are studied by finite-element numerical simulation with the CST microwave studio. As the underlying Pt film hinders the transmission of all light, the absorptivity $A(w)$ is calculated by $A(w) = 1 - |S_{11}|^2$, where S_{11} is the reflection coefficient. The simulation shows that all absorbers each exhibit a strong absorption with a peak absorptivity close to unity. For a configuration with either the larger (configuration S1) or small (configuration S2) resonator alone, the absorption peaks are relatively narrow. Nevertheless, combining the two types of resonators into an integrated one (configuration SM) leads to a broader absorption of 230 GHz with the absorption amplitude over 90%. More simulations further indicate that the absorption spectrum is broadened as the dimension difference between the two size squares increases. At the same time, the small dip between the two peak absorptions becomes undesirably deeper. On the contrary, with the reduction of the dimension difference between the two squares, the absorption top becomes much flatter while the bandwidth decreases correspondingly.

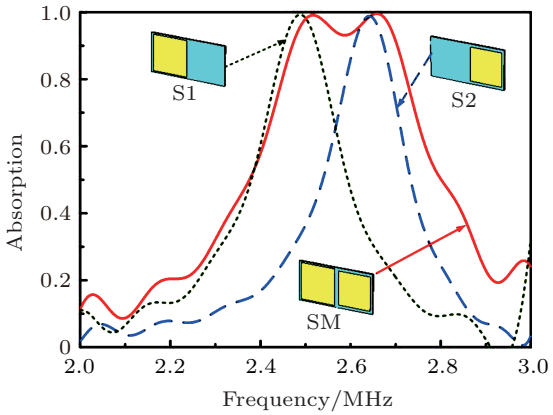


Fig. 2. (color online) Simulated absorption spectra for the three device configurations indicated in the insets.

The distributions of the electric energy density (absorption) of the THz wave are calculated and compared for three specific frequencies, which are shown in Fig. 3. For the low-frequency absorption peak at $f_{S1} = 2.508$ THz, the absorption mainly takes place in a large square (square-1). As to the high-frequency absorption at $f_{S2} = 2.637$ THz, most of the power absorption occur in a small square (square-2). For the absorption dip at $f_{SM} = 2.573$ THz, the absorption occurs in both square-1 and square-2 as expected. It is reasonable to conclude that the absorption at the frequency between f_{S1} and f_{S2} (the grey-shaded area in Fig. 3(d)) is a superposition of the absorptions from both squares. Therefore, if we keep the period (p) of the unit cell unchanged, the dimensions of the metal squares defines f_{S1} and f_{S2}, and consequently the absorption bandwidth.

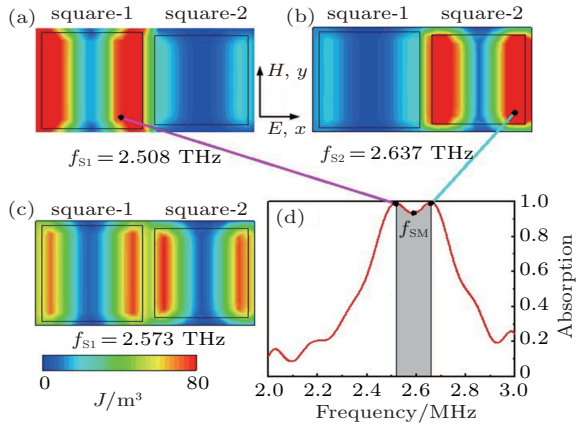


Fig. 3. (color online) Electric energy density distributions at (a) $f_{S1} = 2.508$ THz, (b) $f_{S2} = 2.637$ THz, and (c) $f_{SM} = 2.573$ THz. Panels (a), (b), and (c) share the same color bar. (d) The calculated absorption spectrum of the designed broadband devices.

3. Experiments and discussion

Such a three-layer integrated structure was fabricated using microfabrication techniques. Firstly, a 200-nm-thick Pt/Ti film was e-beam evaporated on Si to form the bottom layer. The SiO_2 dielectric spacer with a thickness of 2 μm was deposited on Pt using plasma enhanced chemical vapor deposition (PECVD). Then a 200-nm-thick Al film was deposited on the top of the SiO_2 film by e-beam deposition. Ultimately, mixed-size Al square arrays were patterned by wet etching with the size parameters defined in Fig. 1(a). A micrograph of a unit cell and a portion of the fabricated absorber are shown in Figs. 1(d) and 1(e). The dimension of the fabricated structure is very close to the theoretically optimized value, and the size parameters are measured and listed in the caption of Fig. 1(e). However, there are still some deviations due to the fabrication tolerances. For example, both squares are slightly smaller while the period is a little large as compared with the designed structure.

The absorption characteristic of the sample was tested using a Fourier transform infrared spectrometer (FTIR) in a reflection geometry. The reflection coefficient measurement was taken with a THz beam in the reflection mode at 30° incidence angle with respect to the normal direction, using a blank Pt coated substrate as the reference. A detailed description of this system can be found in Ref. [32]. The total sample area for measurement was 1.5 cm×1.5 cm to prevent the beam from clipping. Measurements were conducted in a dry-air environment to mitigate the effects of water vapor absorption. The measured absorption as a function of the frequency is displayed in Fig. 4. Two absorption maxima around 2.58 THz and 2.65 THz are clearly observed with absorptions of 99.8% and 98.7%, respectively, between which the minimum absorption in the dip is still as high as 91.8%. The width of the absorption top is 210 GHz if a strict criterion of 90% of the maximum absorption is defined, confirming that broadband absorption was realized in our fabricated absorber.

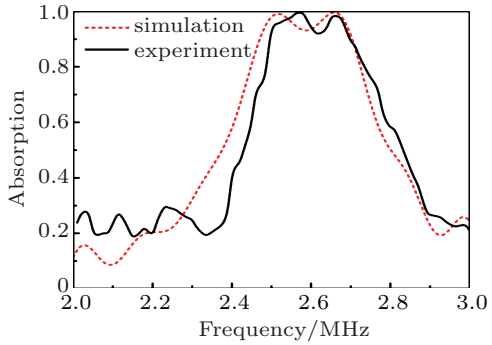


Fig. 4. (color online) Measured (solid curve) and simulated (dash curve) absorption spectra of the MM absorber.

Importantly, the measured absorption curve is clearly consistent with the simulation results, indicating that the adoption of the SiO_2 layer notably improves the simulation accuracy. Simulated results (not shown) indicate that the absorption magnitude suffers a sharp decline if the thickness of the SiO_2 layer deviates from the optimized value. This is because the impedance match between the device and air is broken and consequently gives rise to stronger reflection. Therefore, the excellent agreement between the simulated results and measured values of the absorption amplitude strongly suggests that the fabrication tolerance of SiO_2 film is very small. From Fig. 4, a very small shift of the curve toward high frequency was observed. Tao *et al.*[3] proposed that the absorption frequency of the MM absorber is closely related to the *LC* resonance of the MM. As is well known, the resonance frequency of MM can be expressed as

$$f = \frac{1}{2\pi\sqrt{LC}},$$

where L and C are the inductance and capacitance of the MM resonators. For the square resonators studied here, the equivalent inductances are proportional to their side lengths. It is clear that with the decrease of the side length of the square (thus the reduced L), the resonant frequencies shift towards a higher frequency. Therefore, the slightly blue-shift of the absorption curve of our absorber can be nicely explained since the actual size of the squares is a little smaller than the optimized one, as indicated in Fig. 1.

The polarization property of the absorber was further studied by characterizing the dependence of the absorption on the azimuthal angle (ϕ), as indicated in Fig. 5. The THz source used for the measurement was an optically pumped SIFIR-50 laser made of Coherent-DEOS. A 2.52-THz radiation is generated by pumping CH_3OH (methanol) vapor with a CO_2 laser, producing approximately 140 mW of output power. The measurement was taken with the THz beam in the reflection mode at a 30° incidence angle with respect to the normal direction of the sample plane as indicated in the inset of Fig. 5(b). A

Pyroelectric Camera (Pyroscan III, Ophir-Spiricon Inc) with 124×124 arrays was used as the detector. The sample was mounted on a rotatable test platform, which was carefully calibrated by a blank Pt coated substrate to ensure the complete reception of the reflective THz signals without clipping. Taking the Pt film as a reference, the spatial profile of the reflective signal from our device was recorded by rotating the sample through 360° in steps of 30°, as shown in Fig. 5(a). It can be seen that for the azimuthal angle ϕ ranging from $-90°$ to 90°, the reflection variations of the THz wave are very weak and almost independent of the azimuthal angle. For larger angles of $|\phi| > 90°$, the reflection signals slightly increase with the increase of angle. The absorption magnitudes were calculated for all measured azimuthal angles, and they are summarized in Fig. 5(b). It shows that when we increase the azimuthal angle ϕ from 0° to $(\pm)90°$, the absorption magnitudes show a tiny decrease from 95.4% to 93.4%. With the further increase of ϕ, the absorption decreases a little more, and the minimum absorption of 80% was observed when the THz waves were incident on the structure at $\phi = 180°$ (or $-180°$). Therefore, it can be concluded that the fabricated broadband THz MM absorber is only slightly polarization-sensitive (due to the asymmetric structure), and can be operated well over a large range of azimuthal angles for THz radiation.

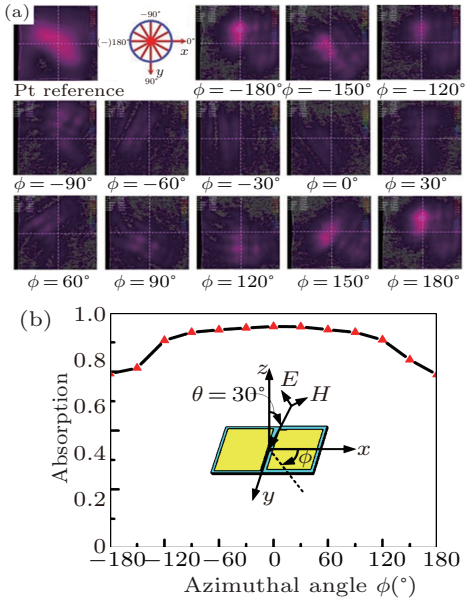


Fig. 5. (color online) (a) Spatial profiles of THz reflection from a blank Pt film reference and our sample with azimuthal angle ϕ ranging from $-180°$ to 180°, and the inset that shows the definition of the value of azimuthal angle. (b) Absorption amplitude as a function of azimuthal angle ϕ, when incident angle $\theta = 30°$.

4. Conclusion

In this paper, a broadband THz absorber using SiO_2-based metamaterial structures is designed and experimentally realized. The bandwidth of the absorption top is 210 GHz even if we define a strict criterion of 90% of the maximum absorption. The measured results show that the MM absorber is only a little polarization-sensitive and can be operated well over a large range of azimuthal angle for THz radiation. This research confirms the possibility of attaining high and broadband absorption by adopting mixed-size metamaterials with an SiO_2 dielectric layer.

References

[1] Schurig D, Mock J J, Justice B J, Cummer S A, Pendry J B, Starr A F and Smith D R 2006 *Science* **314** 977
[2] Tao H, Padilla W J, Zhang X and Averitt R D 2011 *IEEE J. Sel. Top. Quantum Electron.* **17** 92
[3] Tao H, Landy N I, Bingham C M, Zhang X, Averitt R D and Padilla W J 2008 *Opt. Express* **16** 7181
[4] Avitzour Y, Urzhumov Y A and Shvetset G 2009 *Phys. Rev. B* **79** 045131
[5] Landy N I, Sajuyigbe S, Mock J J, Smith D R and Padilla W J 2008 *Phys. Rev. Lett.* **100** 207402
[6] Tao H, Bingham C M, Strikwerda A C, Pilon D, Shrekenhamer D, Landy N I, Fan K, Zhang X, Padilla W J and Averitt R D 2008 *Phys. Rev. B* **78** 241103(R)
[7] He X J, Wang Y, Wang J, Gui T and Wu Q 2011 *Progress in Electromagnetics Research* **115** 381
[8] Grant J, Ma Y, Saha S, Lok L B, Khalid A and Cumming D R S 2011 *Opt. Lett.* **36** 1524
[9] Lu L, Qu S B, Xia S, Xu Z, Ma H, Wang J F and Yu F 2013 *Acta Phys. Sin.* **62** 013701 (in Chinese)
[10] Brown J R, Hibbins A P, Lockyear M J, Lawrence C R and Sambles J R 2008 *J. Appl. Phys.* **104** 043105
[11] Gu C, Qu S B, Pei Z B, Xu Z, Liu J and Gu W 2011 *Chin. Phys. B* **20** 017801
[12] Wen Q Y, Zhang H W, Xie Y S, Yang Q H and Liu Y L 2009 *Appl. Phys. Lett.* **95** 241111
[13] Shen X P, Cui T J and Ye J X 2012 *Acta Phys. Sin.* **61** 058101 (in Chinese)
[14] Chen Z and Zhang Y X 2013 *Chin. Phys. B* **22** 067802
[15] Huang L and Chen H 2011 *Progress in Electromagnetics Research* **113** 103
[16] Peng X Y, Wang B, Lai S M, Zhang D H and Teng J H 2012 *Opt. Express* **20** 27756
[17] Ye Y Q, Jin Y and He S 2010 *J. Opt. Soc. Am. B* **27** 498
[18] Cheng Y Z, Nie Y and Gong R Z 2013 *Opt. Laser Technol.* **48** 415
[19] Hu C G, Liu L Y, Zhao Z Y, Chen X N and Luo X G 2009 *Opt. Express* **17** 16745
[20] Wakatsuchi H, Greedy S, Christopoulos C and Paul J 2010 *Opt. Express* **18** 22187
[21] Luo H, Cheng Y Z and Gong R Z 2011 *Eur. Phys. J. B* **81** 387
[22] Alici K B, Turhan A B, Soukoulis C M and Ozbay E 2011 *Opt. Express* **19** 14260
[23] Grant J, Ma Y, Saha S, Khalid A and Cumming D R S 2011 *Opt. Lett.* **36** 3476
[24] Huang L, Chowdhury D R, Ramani S, Reiten M T, Luo S N, Taylor A J and Chen H T 2012 *Opt. Lett.* **37** 154
[25] Grbovic D, Lavrik N V, Rajic S and Datskos P G 2008 *J. Appl. Phys.* **104** 054508
[26] Alves F, Kearney B, Grbovic D, Lavrik N V and Karunasiri G 2012 *Appl. Phys. Lett.* **100** 111104
[27] Gunde M K and Macek M 2001 *Phys. Status Solidi A* **183** 439
[28] Smith D Y, Shiles E and Inokuti M 1998 "The Optical Properties of Metallic Aluminum," in *Handbook of Optical Constants of Solids*, ed. E. D. Palik (Boston: Academic Press)
[29] Shchegolkov D Y, Azad A K, O'Hara J F and Simakov E I 2010 *Phys. Rev. B* **82** 205117
[30] Zhu W R and Zhao X P 2009 *J. Opt. Soc. Am. B* **26** 2382
[31] Ding F, Cui Y X, Ge X C, Jin Y and He S L 2012 *Appl. Phys. Lett.* **100** 103506
[32] Bolakis C, Grbovic D, Lavrik N V and Karunasiri G 2010 *Opt. Express* **18** 14488